이학석사 학위논문

SCAMP5/AP-4 dependent trafficking mediates presynaptic localization of the core autophagy protein ATG9A

SCAMP5와 AP-4 상호작용에 의한 자가포식 핵심단백질 ATG9A의 시냅스 위치화에 대한 연구

2023년 8월

서울대학교 대학원

협동과정 뇌과학전공

류 승 현

SCAMP5/AP-4 dependent trafficking mediates presynaptic localization of the core autophagy protein ATG9A

지도 교수 장 성 호

이 논문을 이학석사 학위논문으로 제출함
2023년 8월

서울대학교 대학원
협동과정 뇌과학전공
류 승 현

류승현의 이학석사 학위논문을 인준함
2023년 8월

위 원 장 _____ 최 명 환 _____ (인)

부위원장 _____ 장 성 호 _____ (인)

위 원 _____ 김 형 _____ (인)

Abstract

Secretory carrier membrane protein 5 (SCAMP5) is a transmembrane protein that is highly expressed in the brain and predominantly localized to synaptic vesicles (SVs). As a key regulator of synaptic function in neurons, recent studies have shown that SCAMP5 is involved in the regulation of SV endo/exocytosis and protein trafficking, particularly at the axon and presynaptic localization. Moreover, studies have shown that SCAMP5 is not only enriched in SVs but also highly expressed in the Golgi network. However, unlike studies that have established its role at the synapse, it is unclear why SCAMP5 is located in the Golgi network.

The initial insight came from my experiments, in which I found that depletion of SCAMP5 resulted in aberrant autophagosome formation at presynaptic boutons. I performed a co-immunoprecipitation analysis and revealed that SCAMP5 directly binds to adapter protein 4 (AP-4), especially the μ4 subunit of AP-4 (AP4M1). Protein-protein interaction analysis using truncated constructs has revealed that AP4M1 directly associates with the N-terminal region of SCAMP5. Immunocytochemistry and fluorescent imaging analysis have revealed that the interaction between SCAMP5 and AP4M1 plays a key role in the recruitment of AP-4 to the trans-Golgi network (TGN). AP-4 is known to play a critical role in vesicle-mediated protein transport by selecting and packaging cargo at the TGN, and one of the AP-4-mediated export cargoes is a core autophagy

protein ATG9A. I found that either the shRNA-mediated knockdown (KD) of SCAMP5 or the disruption of SCAMP5/AP4M1 interaction resulted in a significant decrease in the axonal trafficking of ATG9A vesicles into presynaptic terminals. It subsequently led to impaired presynaptic autophagy and reduced turnover of SV proteins at the presynaptic terminals.

The results of this study suggest that SCAMP5 through direct interaction with AP-4, plays a critical role in the recruitment of AP-4 to the TGN and subsequently regulates the axonal trafficking and synaptic localization of ATG9A. Given the established correlation of both SCAMP5 and autophagy deficiency in neurodevelopmental disorders, conducting further investigations offers a valuable opportunity to elucidate the complex molecular mechanisms underpinning the pathogenesis of these conditions.

Keyword: SCAMP5, AP-4, ATG9A, presynapse, axonal trafficking, autophagy

Student Number: 2021-22014

Table of Contents

SCAMP5/AP-4 dependent trafficking mediates presynaptic localization of the core autophagy protein ATG9A

Introduction

Secretory carrier membrane proteins (SCAMPs), a family of ubiquitous tetraspanning vesicle membrane proteins, are known to function in vesicular trafficking and recycling processes. Among five SCAMPs (SCAMP1~5), SCAMP1 and SCAMP5 are highly expressed in the brain and synaptic vesicle (SV) [1]. However, studies have shown that knockout of SCAMP1 does not result in defects in neural function, whereas SCAMP5 appears to be a critical protein in the regulation of synaptic function [2]. Recent research has highlighted the significance of SCAMP5 deficiency in the pathogenesis of various neurodevelopmental diseases such as autism, pediatric epilepsy, and Parkinson's disease [3-5]. This is attributed to the critical role of SCAMP5 in SV endocytosis during high neuronal activity conditions [6], regulating short-term depression of SV exocytosis through clearance of release sites [7], and axonal trafficking and synaptic localization of NHE6 to modulate quantal size at glutamatergic synapses [8].

Adapter protein (AP) complexes are heterotetrameric proteins composed of four subunits: 4 subunits: two large subunits (β1-5, and either α, γ, δ, ϵ or ζ), one medium subunit (μ1-5) and one small subunit (σ1-5). They play a key role in the vesicular trafficking of transmembrane proteins. While five members of AP complexes have been identified, AP-1 and AP-2 are well-known for their functions as a bridge between clathrin and transmembrane proteins, aiding in the formation of clathrin-coated vesicles [9]. On the other hand, AP-4 and AP-5 are independent of clathrin and have been implicated in various cellular processes, including lysosomal biogenesis, protein sorting in the TGN, and vesicular transport [10-13]. Mutations in any of the subunits of AP-4, including β4 (AP4B1), ϵ4 (AP4E1), μ4 (AP4M1), and σ4 (AP4S1) lead to AP-4 deficiency syndrome, also known as AP-4 associated hereditary spastic paraplegia (HSP). This condition is

associated with a range of disorders, such as developmental delay, intellectual disability, and epilepsy [10, 14–16], but the underlying physiological mechanisms of these conditions remain poorly understood.

Autophagy is a protein–degradative pathway that maintains cellular homeostasis, growth, differentiation, and development [17–20]. The process involves the formation of a pre–autophagosomal structure known as the phagophore or isolation membrane, which eventually matures into an autophagosome. The autophagosome then fuses with lysosomes, leading to the degradation and recycling of proteins. Autophagy requires more than 30 proteins to complete all its steps, and autophagy–related (ATG) proteins serve as critical markers for the identification and characterization of each step in the autophagy process [21]. Among the ATG proteins, ATG9A, the only transmembrane protein in the autophagy pathway, plays a vital role in the initiation of phagophore formation. ATG9A is located in the somatodendrites, axons, and axon terminals, where it plays a key role in generating autophagosomes through vesicular transport from the trans–Golgi network (TGN) [22, 23]. Recent studies have suggested that ATG9A localizes at the presynaptic terminal by AP–4 exportation [24, 25]. Nevertheless, the complete pathway and underlying mechanisms regulating the localization of ATG9A at presynaptic terminals remain elusive, and further studies are needed to elucidate the exact details of this process.

In this study, I found that SCAMP5 is significantly enriched at both presynaptic boutons and the Golgi network in rat hippocampal neurons. Importantly, the downregulation of SCAMP5 resulted in impaired autophagosome formation at presynaptic boutons, indicating a critical role for SCAMP5 in presynaptic autophagy. Further investigation revealed that the N–terminal region of SCAMP5 directly interacts with AP4M1. The absence of SCAMP5 disrupts the localization of AP–4 at the TGN, impeding the proper targeting of ATG9A to presynaptic boutons. The failure in

presynaptic localization of both overexpressed and endogenous ATG9A is correlated with its accumulation at the TGN. The observed defects in SCAMP5 knockdown were also evident in neurons with AP4M1 knockout, indicating that the presynaptic localization of ATG9A is mediated by the interaction between SCAMP5 and AP4M1. In addition, the knockdown of SCAMP5 led to the accumulation of an older pool of synaptic vesicle proteins, indicating defects in autophagy and protein turnover at the presynaptic terminals.

Taken together, the findings from this study underscore the significance of the interaction between SCAMP5 and AP4M1 at TGN in regulating the presynaptic localization of ATG9A. The disruption of this interaction leads to defects in the transport of ATG9A and subsequent autophagosome formation at presynaptic boutons, thus impairing protein turnover at the presynaptic terminals. My study further proposes that targeting SCAMP5's role in presynaptic autophagy holds promise as a potential therapeutic approach for addressing presynaptic autophagy-related disorders.

Materials and Methods

Plasmid DNA Construction

Full-length or domain fragments of GFP-tagged rat SCAMP5 cDNA (NM-031726) constructs and small hairpin RNA (shRNA) for SCAMP5 were made as previously reported [6-8]. Missense or nonsense mutation of SCAMP5 constructs was made by site-directed mutagenesis. AP4M1-HA construct was generated by insertion of the HA epitope at the C-terminal region of the human AP4M1 cDNA (purchased from Korea Human Gene Bank, Medical Genomics Research Center, KRIBB, Korea). The target sequence for AP4M1 knockout (KO) based on CRISPR/Cas9 system was predicted by CCTOP [26]. sgRNA–targeting AP4M1 exon 1: 5'-CCTTCTTGTCTTACTTCTTGA-3'- was cloned into pSpCas9(BB)-2A-GFP(PX458-GFP) purchased from Addgene (Plasmid #48138) as described in the Zhang Lab General Cloning Protocol [27].

The following plasmids were generously provided: GFP-Synaptophysin (from Dr. Jane Sullivan, University of Washington), mNeongreen-Giantin (from Dr. Dorus Gadella, Addgene Plasmid #98880), pMXs-puro-RFP-ATG9A (from Dr. Noboru Mizushima, Addgene Plasmid #60609), and FU-mFT-SV2 (from Dr. Craig Garner, German Center for Neurodegenerative Diseases (DZNE)).

Antibodies

Anti-rabbit SCAMP5 (ab3432; Abcam), Anti-mouse synaptophysin 1 (101 011; Synaptic Systems), Anti-mouse EEA1 (610456; BD Biosciences), Anti-mouse LAMP1 (MA1-164; Invitrogen), Anti-mouse TGN38 (610898; BD Biosciences), Anti-rabbit TGN38 (NBP1-03495; Novus Biologicals), Anti-rabbit LC3B (L7543; Sigma), Anti-rabbit AP1M1 (ap50198pu-n; ACRIS), Anti-mouse AP2M1 (611350; BD Biosciences), Anti-rabbit AP4M1 (PA5-22380; Invitrogen), Anti-rabbit β-tubulin (ab6046; Abcam), Anti-mouse HA (901514; BioLegend), Anti-mouse AP4E1 (612018; BD

Biosciences), Anti-rabbit ATG9A (ab108338; Abcam), Anti-rabbit Arf1 (PA1-127; Invitrogen), and Anti-mouse SQSTM1/p62 (ab56416; Abcam) were used in the experiments. Anti-rabbit GFP antibody was custom-made by affinity purification by our laboratory. All horseradish peroxidase-conjugated secondary IgG antibodies (Jackson ImmunoResearch) and Alexa Fluor secondary antibodies (Thermo Fisher Scientific) were used respectively in each experiment.

Cell lines culture and transfection

HEK-293T and HT-22 cell lines were maintained in Dulbecco's Modified Eagle's Medium containing 10 % fetal bovine serum (FBS), 100 U/ml penicillin, and 100 μg/ml streptomycin at 37 °C in 5 % CO2 humidified incubator.

Cells were transfected by PEI-MAX (MW 40,000). For 90 mm culture dishes, 10 μg of plasmid DNA were added to Opti-MEM each and mixed briefly, followed added 30 μg PEI-MAX (1:3 ratio) and incubated for 20 min. After incubation, the transfection mixture was added to cells for 3 hr and replaced with fresh complete medium.

Rat primary hippocampal neuron culture and transfection

For primary hippocampal neuron culture, the fetal Sprague Dawley rats (at embryonic day 18) were euthanized by CO2 for dissection of the hippocampus. Embryonic hippocampi were treated with papain and DNase in HBSS at 37 °C and dissociated in plating medium (minimum essential medium (MEM), 0.6 % glucose, 1 mM sodium pyruvate, 2 mM GlutaMax (Gibco), and 10 % FBS) after trituration with polished half-bore Pasteur pipettes. Approximately 40,000 cells were plated onto poly-D-lysine-coated 18 mm glass coverslips in 60 mm dishes. After 3 hr, the plating medium was replaced with the neurobasal medium (Invitrogen) containing 2 % B-27 supplement (Invitrogen), 0.5 mM GlutaMax, and 1 μM

Cytosine 1-β-D-arabinofuranoside (Ara-C; Sigma-Aldrich). Cells were maintained at 37 °C in a 5 % CO2 humidified incubator, and half of the medium was replaced with the fresh complete neurobasal medium at DIV 4, 7, and 14. All animal experiments were performed according to the Institute of Animal Care and Use Committee guidelines of Seoul National University (SNU-220525-4).

Hippocampal neurons were transfected at DIV 7-10 using the calcium phosphate method. 9 μg of plasmid DNA and 10 μl of 2.5 M $CaCl_2$ were mixed in distilled water (Final volume: 75 μl) and added to the equal volume of 2x BBS (50 mM BES, 280 mM NaCl, and 1.5 mM Na_2HPO_4; pH 7.1). The mixture was incubated for 20 min at room temperature and then added to neurons in transfection medium (MEM, 0.6 % glucose, 1 mM sodium pyruvate, 10 mM GlutaMax (Gibco), and 10 mM HEPES; pH 7.65) for 1 hr at 37 °C. After 1 hr, the medium was replaced with washing medium (MEM, 0.6 % glucose, 1 mM sodium pyruvate, 10 mM GlutaMax, and 10 mM HEPES; pH 7.35) for 30 min at 37 °C and again replaced with the original complete neurobasal medium.

Immunocytochemistry

Cultured rat hippocampal neurons were fixed in 4 % paraformaldehyde with 4 % sucrose in PBS for 10 min at room temperature (RT). Then, neurons were washed three times by PBS-G (50 mM glycine in PBS) and blocked with 10 % normal goat serum (NGS) and 0.1 % Tx-100/PBS for 1.5 hr at RT. Neurons were incubated with respective primary antibodies diluted in blocking solution (5 % NGS and 0.1 % Tx-100/PBS) overnight at 4 °C, followed by secondary antibodies incubated with blocking solution for 45 min at 37 °C. After immunostaining, coverslips were finally washed again and mounted on a sliding glass with an aqueous mounting medium (Dako).

Western blot and immunoprecipitation

Cells were lysed with 1 % Triton X-100 lysis buffer (20 mM Tris-HCl (pH 8.0), 1 % Triton X-100, 10 % Glycerol, 137 mM NaCl, 2 mM EDTA, 1 mM PMSF, and 1x protease inhibitor cocktail (Sigma)). Cell lysates were centrifuged at 14,000 xg for 20 min at 4 °C after sonication and collected only supernatants for samples. Obtained lysates were mixed with 2x or 5x protein sample buffer and boiled for 5 min at 100 °C. For the blotting of ATG9A protein, samples were not subjected to boiling to prevent protein aggregation caused by the transmembrane nature of ATG9A. Each sample was loaded onto Tris-glycine gels (6-12 %) and transferred to 0.45 μm PVDF membranes (Pall Life Sciences). After protein transfer, membranes were blocked with 5 % skim milk diluted in TBS-T (Tris-buffered saline with 0.1 % Tween-20) for 30 min and incubated with respective primary antibody for overnight at 4 °C. After 3 times washing by TBS-T, membranes were incubated with appropriate horseradish peroxidase (HRP)-conjugated secondary antibody for 45 min at RT. The chemiluminescence signals were developed by an enhanced chemiluminescence reagent (AbClon) and detected with Amersham Imager 680 (GE Healthcare).

For immunoprecipitation, the same amounts of protein (500-1000 μg) were incubated with primary antibody overnight at 4 °C. After incubation, Protein A-Sepharose beads (GE Healthcare) or Pierce Protein A/G Magnetic beads (Thermo Scientific) as related to experiment for 2 hr at 4 °C and washed 3 times with lysis buffer. Beads were eluted with 2x protein sample buffer and boiled for 5 min at 100 °C. The following procedures were the same as the western blotting protocol.

Adeno-associated virus (AAV) production

HEK-293T cells were triple transfected with an inverted terminal repeat (ITR) vector containing the gene of interest, pAAV-DJ (Cell Biolabs) and pHelper (Cell Biolabs) in a 1:1:1 molecular weight ratio. The transfection was performed using PEI and the cells were

harvested 48–72 hours after transfection. Cell pellets were resuspended in phosphate-buffered saline (PBS) and subjected to four rounds of freezing and melting with a cooling and warming bath. The AAVs were purified using polyethylene glycol 8000 (PEG 8000)–NaCl and extracted with chloroform to remove hydrophilic proteins and PEG residues. After 30 min of incubation to remove chloroform, the collected AAVs were concentrated using dialysis tubes and stored at −80 °C. Genomic titers of AAV were determined using the StepOne Real-Time PCR System (Applied Biosystems), and 10 multiplicities of infection (MOI) of AAV were used for infection.

Fluorescence imaging and statistical analysis

For live cell imaging, neurons at DIV 14–16 were imaged in Tyrode's solution (136 mM NaCl, 2.5 mM KCl, 2 mM $CaCl_2$, 1.3 mM $MgCl_2$, 10 mM glucose, 10 mM HEPES; pH 7.4, 285–290 mOsm) using a Nikon spinning disk confocal microscope (CSU-X1, Nikon) equipped with a 40X oil-immersion objective lens (Plan Apo NA 1.30) and a Neo sCMOS camera (Andor Technology) driven by NIS-Elements software. All other images were acquired using ZEISS laser scanning microscope LSM980 (Carl Zeiss, Jena, Germany) equipped with a 63X oil-immersion objective lens (Plan-Apochromat 1.4) and an AxioCam305 mono camera (Carl Zeiss) driven by Zen blue 3.4 software, or a spinning disk confocal microscope as described above.

To analyze protein colocalization, Mander's colocalization coefficients (MCCs) were calculated with ImageJ (NIH) and JACoP plugin (https://imagej.nih.gov/ij/plugins/track/jacop2.html). All values are presented as the mean ± SEM. The average MCC value of each sample was compared using either a student's t-test or a one-way ANOVA followed by Tukey's post hoc test. The significance of all data is reported as $*p < 0.05$, $**p < 0.01$, $***p < 0.001$.

Results

N-terminal region of SCAMP5 binds to AP4M1 at the trans-Golgi network

SCAMPs are known to be distributed across synaptic vesicles, secretion granules, transporter vesicles, endosomal compartments, and Golgi membranes [8, 28-31]. To investigate the distribution of SCAMP5, I first performed immunocytochemistry (ICC) and fluorescence imaging in the primary rat hippocampal neurons (Figures 1A and B). SCAMP5 is significantly enriched at presynaptic boutons and also highly distributed at the Golgi network. This phenomenon is specific to SCAMP5 and not observed in another synaptic vesicle protein (Figures 2A and B), suggesting that SCAMP5 plays a distinct role with the Golgi network in neuronal cells.

Through further investigations, I observed that the downregulation of SCAMP5 in hippocampal neurons resulted in impaired autophagosome formation, especially at presynaptic boutons. Treatment with 2 μM rapamycin, a widely recognized inducer of autophagy in neuronal cells [32], promoted the formation of autophagosomes at the presynaptic boutons in hippocampal neurons. In contrast, the downregulation of SCAMP5 with previously validated short hairpin RNA (shRNA) to knockdown (KD) SCAMP5 expression [6-8], led to a significant reduction of autophagosome formation (Figures 3A and B). Notably, this defective phenomenon was observed across the overall population of boutons, rather than being limited to a subset (Figure 3C). These findings were further supported by the increased expression of LC3-II, an autophagic marker, in both control and SCAMP5 knockdown neurons upon rapamycin treatment (Figures 4A and B), indicating that SCAMP5 knockdown especially impairs autophagosome formation at the presynaptic boutons. The observed phenomena are also evident during activity-dependent induction of autophagy by 90 mM high KCl (Figures 5A-C), emphasizing the crucial role of SCAMP5 in facilitating presynaptic autophagosome formation.

Autophagy initiation and expansion of phagophores depends on the cargo, and the source of membrane, which are derived from the endoplasmic reticulum, Golgi, and plasma membrane [33-35]. Additionally, previous studies have shown that the adapter protein 4 (AP-4) located at the trans-Golgi network (TGN) plays important role in regulating autophagy in axons [24, 25]. To establish a

connection between SCAMP5 at the Golgi network and autophagy, I investigated the potential interaction between SCAMP5 and AP-4. Co-immunoprecipitation assay was performed, which revealed that SCAMP5 interacts with μ4 subunit of AP-2 (AP2M1), as previously found [7], and with AP-4 (AP4M1) in the rat hippocampal neurons, but not with AP-1 (AP1M1) (Figures 6A-C). This interaction was observed to have high colocalization at the TGN (Figures 7A and B). To identify the binding domain of SCAMP5 with AP4M1, another co-immunoprecipitation assay was performed (Figure 8A). Despite the interaction between SCAMP5 and AP4M1, none of the cytosolic domains of SCAMP5 (Nt cyto, 2/3 cyto, and Ct cyto) interacted with AP4M1 (Figure 8B). However, the N-terminal region containing the first transmembrane region (Nt-TM1) was found to be responsible for binding to AP4M1, while the C-terminal region containing the fourth transmembrane region (TM4-Ct) and 2/3 loop flanked by a transmembrane region at both N- and C- termini (TM2-2/3-TM3) did not show any binding affinity (Figure 8C), indicating that the transmembrane domain is also crucial for AP4M1 binding to the N-terminal region of SCAMP5. To confirm the importance of the N-terminal region of SCAMP5 for its interaction with AP4M1, an experiment conducted using a mutant form of SCAMP5 lacking the N-terminal region (ΔNt), which revealed a lack of interaction with AP4M1 (Figure 8D). Collectively, these results indicate a direct binding between AP4M1 and the N-terminal region of SCAMP5 at the TGN.

SCAMP5/AP4M1 interaction mediates AP-4 localization at the trans-Golgi network

Although AP-4 is known to be important for cargo export from the TGN [10, 11], there is still limited research on the recruitment mechanism of AP-4 to the TGN. Given the interaction between SCAMP5 and AP-4 at the TGN, I hypothesized that SCAMP5 plays a role in recruiting AP-4 to the TGN. To test this hypothesis, I performed ICC to visualize the location of AP-4 upon downregulation of SCAMP5 in rat hippocampal neurons. Due to the unavailability of commercial antibodies for the detection of endogenous AP4M1, I use an antibody against the AP4E1 to observe the localization of endogenous AP-4 for ICC. The results showed that AP-4 localized predominantly at the TGN, and the downregulation of SCAMP5 significantly reduced the amount of AP-4 in the cell body and its recruitment to the TGN (Figures 9A-D). These results further suggest that the interaction between SCAMP5 and AP4M1 is essential for the proper localization of AP-

4 at the TGN.

Knockdown of SCAMP5 or disruption of SCAMP5/AP4M1 interaction interferes with the axonal trafficking and presynaptic localization of ATG9A

Recent studies have shown that the autophagy-related protein 9A (ATG9A) is an essential protein for presynaptic autophagy, which is facilitated by cargo transport from the TGN via the AP-4 complex in mammals [24, 25, 36]. Downregulation of SCAMP5 has been shown to result in defective autophagosome formation at presynaptic boutons (Figures 3 and 5), and the recruitment of AP-4 to the TGN is mediated by SCAMP5 (Figure 9). Based on the hypothesis that SCAMP5 regulates the trafficking pathway of AP-4/ATG9A for presynaptic autophagy, I conducted co-transfection of ATG9A and SYP, a presynaptic bouton marker, with scrambled RNA or shRNA targeting SCAMP5 in rat hippocampal neurons (Figures 10A, B and D). In SCAMP5 knockdown neurons, I observed impairments specifically in the trafficking of ATG9A vesicles to the axon, while the localization of SYP remained unaffected. Furthermore, there was a reduced localization of ATG9A to presynaptic boutons in SCAMP5 knockdown neurons (Figures 10E-G), and expressing a shRNA-resistant form of wild-type SCAMP5 (SC5 RES) fully rescued observed impairments in ATG9A trafficking and localization to presynaptic boutons (Figures 10C-G).

To address concerns regarding potential artifacts resulting from ATG9A overexpression, I then performed ICC to examine the endogenous localization of ATG9A in control, SCAMP5 KD, and AP4M1 KO neurons. To achieve knockout (KO) of AP4M1, I employed Clustered Regularly Interspaced Short Palindromic Repeats/Cas9 (CRISPR/Cas9) technology. Especially, I designed a single guide RNA (sgRNA) targeting the first exon of AP4M1 and cloned it into pSpCas9(BB)-2A-GFP (px458) vector [27] (Figure 11A). AP4M1 protein KO by CRISPR/Cas9 was validated by performing immunoblotting (Figures 11B and C) and genomic DNA cleavage surveyor assay [37] (Figure 11D). The sgRNA used for CRISPR/Cas9-mediated KO was designed to target AP4M1, but also effects on the expression of the ε4 subunit of AP-4 (AP4E1) were observed (Figure 11B). The fluorescent images revealed that ATG9A was predominantly localized at the TGN (Figures 12A, E, and F). However, in SCAMP5 KD and AP4M1 KO neurons, there was an increased accumulation of ATG9A in the cell body within the TGN (Figures 12B, C, E, and F). Notably, the accumulation rate of

ATG9A was found to be higher in AP4M1 KO neurons compared to SCAMP5 KD neurons (Figures 12D–F). This observation may be attributed to the 3–4 folding upregulation of ATG9A protein synthesis resulting from the AP–4 protein KO, as reported previously in the literature [25, 38, 39]. Therefore, there is a possibility that downregulation of SCAMP5 may not much impact the expression level of ATG9A protein. To rule out this possibility, immunoblot analysis was performed using neuron lysates from control and SCAMP5 knockdown neurons. Based on the immunoblotting data, the total amount of endogenous ATG9A was found to be 1.5–fold higher in SCAMP5 KD neurons, indicating that SCAMP5 downregulation did not significantly affect the synthesis of ATG9A protein compared to AP–4 KO neurons (Figures 13A and B). To investigate the impact of SCAMP5 or AP4M1 downregulation on endogenous ATG9A localization, I conducted an additional ICC experiment to examine the axonal distribution of endogenous ATG9A. SCAMP5 KD and AP4M1 KO neurons both resulted in defective trafficking of ATG9A in the axon and reduced localization of ATG9A to presynaptic boutons, similar to the effects observed with ATG9A overexpression (Figures 14A–F, G, and H). Furthermore, in double SCAMP5 KD+AP4M1 KO neurons, there was no significant difference in the defective trafficking of ATG9A compared to neurons with SCAMP5 KD or AP4M1 KO alone (Figures 14G–H). This finding confirms that SCAMP5 and AP–4 are involved in the same trafficking for ATG9A. Consequently, I propose that the interaction between SCAMP5 and AP–4 serves as a crucial regulatory mechanism governing the ATG9A trafficking pathway from the TGN to the presynaptic boutons.

Accumulation of older synaptic vesicle proteins in neurons with SCAMP5 knockdown

Due to the involvement of presynaptic autophagy in the removal of old synaptic vesicle (SV) proteins [38, 40], I hypothesized that SCAMP5 plays a role in the recycling pathway of SV protein through the autophagy pathway. To address this possibility, I utilized a medium fluorescent timer (mFT) construct tagged with SV2, a protein of the SV (mFT–SV2) [41]. The mFT–SV2 construct allowed us to monitor the age of the SV protein pool by the change in the fluorescent color from blue to red as time elapsed based on the blue/red fluorescent ratio [42]. I transfected mFT–SV2 in both control and SCAMP5 KD neurons, and results showed that SCAMP5 KD neurons displayed defects in protein turnover of SV proteins at the presynaptic terminals compared to

the control group (Figures 15A and B). The observed accumulated older pool of SV proteins in SCAMP5 KD neurons was not limited to specific boutons but was observed across a broad range of boutons (Figure 15C). These results confirm that the formation of presynaptic autophagosomes, mediated by SCAMP5/AP-4/ATG9A, regulates the recycling of SV proteins at the presynaptic boutons.

Figures

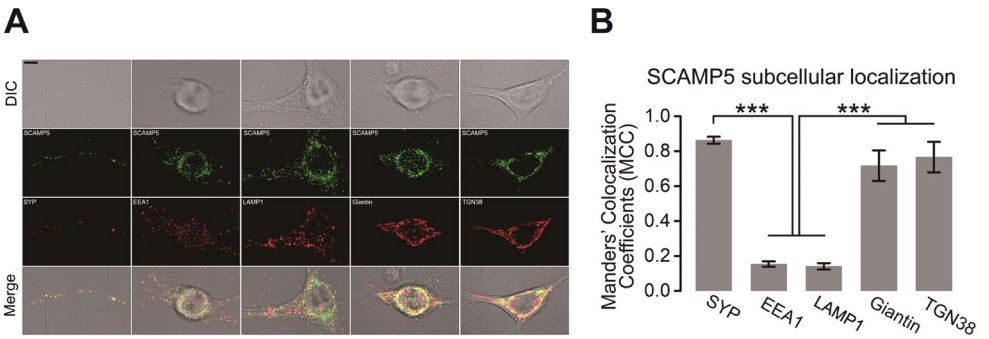

Figure 1. SCAMP5 is highly enriched at both presynaptic boutons and the Golgi network in the rat hippocampal neuron.
(A) Rat hippocampal neurons were subjected to immunostaining using specific antibodies to detect colocalization of endogenous SCAMP5 with various markers. The presynaptic bouton marker, Synaptophysin (SYP), was detected using anti-SYP antibody. The early endosome marker, Early endosome antigen 1 (EEA1), was detected using anti-EEA1 antibody. Lysosomes were detected using anti-Lysosomal-associated membrane protein 1 (LAMP1) antibody, while the trans-Golgi network was detected using anti-TGN38 antibody. Additionally, the cis-Golgi marker, Giantin, was transfected into rat hippocampal neurons to detect the cis-Golgi compartment. The presence of SCAMP5 was detected using anti-SCAMP5 antibody. Scale bar: 5 μm. **(B)** Mander's colocalization coefficients of SCAMP5 overlapping to relative proteins, SCAMP5 overlapping SYP: 0.86 ± 0.04, n = 5 (coverslips); SCAMP5 overlapping EEA1: 0.15 ± 0.04, n = 5 (coverslips); SCAMP5 overlapping LAMP1: 0.14 ± 0.03, n = 5 (coverslips); SCAMP5 overlapping Giantin: 0.72 ± 0.17, n = 5 (coverslips); SCAMP5 overlapping TGN38: 0.76 ± 0.17, n = 5 (coverslips); $F_{(4,20)} = 9.982$, $p < 0.0001$, analyzed by One-way ANOVA followed by Tukey HSD post hoc test. Values are indicated as mean ± SEM. ***$p < 0.001$. DIC: Differential Interference Contrast.

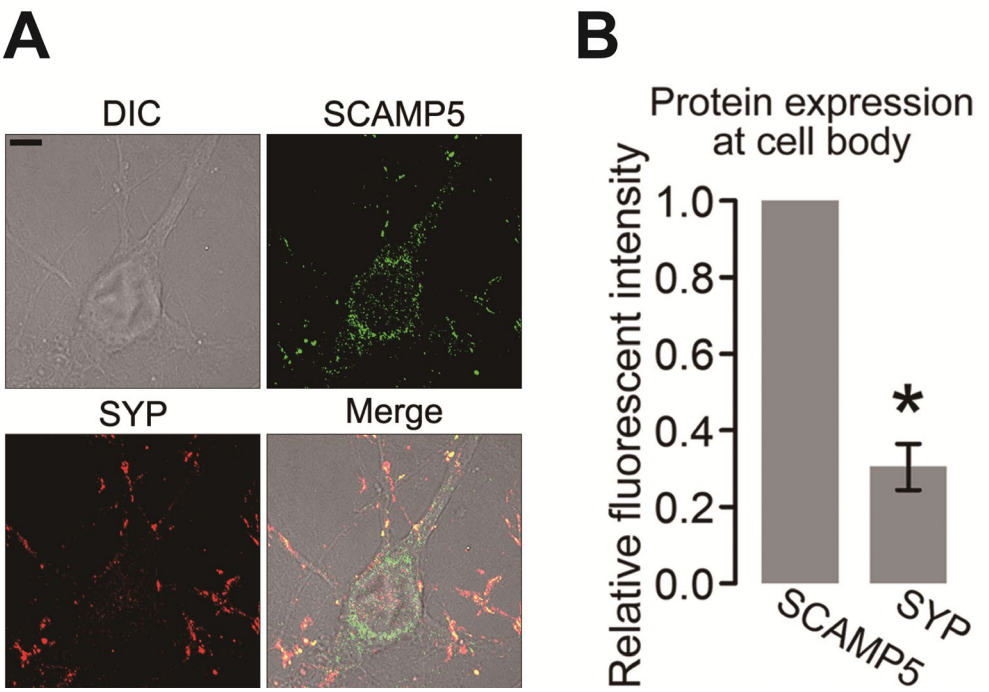

Figure 2. Subcellular localization of synaptic vesicle protein SYP excludes its presence in the cell body, unlike SCAMP5.
(A) Immunostaining of rat hippocampal neurons were anti-SCAMP5 and anti-Synaptophysin (SYP) antibodies. Scale bar: 5 μm. **(B)** Normalized relative cell body intensity of SYP protein expression by SCAMP5 protein expression, SCAMP5: 1.00 ± 0 (normalized), n = 5 (coverslips); SYP: 0.30 ± 0.12, n = 5 (coverslips); p = 0.0282, analyzed by Student's t-test. Values are indicated as mean ± SEM. *$p < 0.05$.

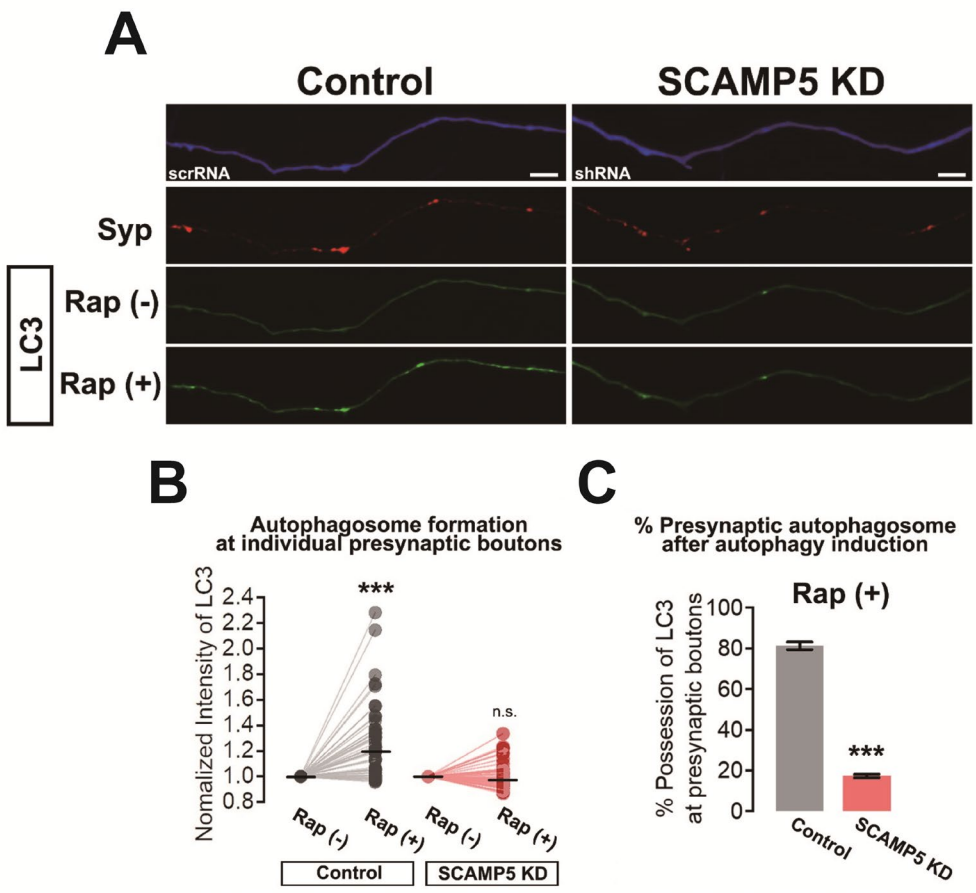

Figure 3. Downregulation of SCAMP5 leads to defective autophagosome formation at presynaptic boutons even in the presence of rapamycin treatment.

(A) Representative images of cultured rat hippocampal neurons co-transfected with mTagBFP2-scrRNA or shRNA of SCAMP5, mCherry-Synaptophysin (SYP; presynaptic bouton marker), and EGFP-LC3 (autophagosome marker) with or without treatment of rapamycin for autophagy induction. Scale bar: 5 μm. (B) Quantification of the normalized relative intensity of LC3 protein expression in control and SCAMP5 KD neurons with or without treatment of rapamycin treatment, Control: Rap (−): 1.000 ± 0.000 (normalized), Rap (+): 1.283 ± 0.002, n = 102 (boutons, 10 coverslips); p = 5.627E−05, analyzed by Student's t-test, SCAMP5 KD: Rap (−): 1.000 ± 0.000 (normalized), Rap (+): 1.014 ± 0.001, n =1 02 (boutons, 8 coverslips); p = 0.320, analyzed by Student's t-test. Values are indicated as mean ± SEM. (C) Percentage of LC3 possession at presynaptic boutons in control and SCAMP5 KD neurons with rapamycin treatment, Control: 81.14 ±

3.85, n=5 (coverslips); SCAMP5 KD: 17.40 ± 1.83, n = 5 (coverslips); $p < 0.0001$, analyzed by Student's t−test. Values are indicated as mean ± SEM. ***$p < 0.001$. KD: knockdown; Rap: rapamycin; scrRNA: scrambled RNA; shRNA: short hairpin RNA.

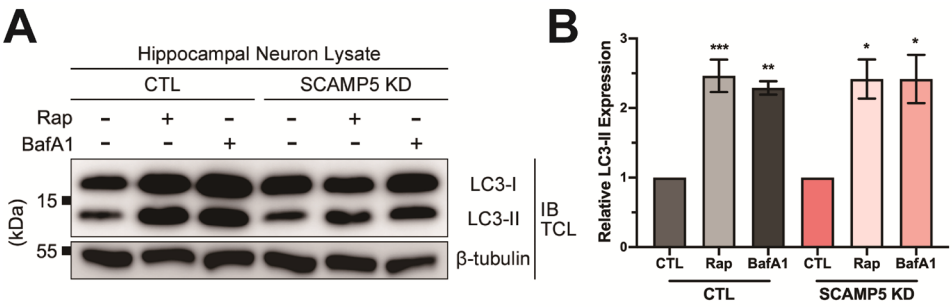

Figure 4. Rapamycin induces autophagy in both control and SCAMP5 knockdown neurons.

(A) Cultured hippocampal neurons were subjected to treatment with AAV containing SCAMP5 scrRNA (CTL) or shRNA (SCAMP5 KD), followed by lysing the cells for immunoblotting analysis with Anti-LC3B antibody before and after treatment with rapamycin (Rap) and bafilomycin A1 (BafA1). (B) Normalized relative band intensity of LC3-II protein expression, Control: CTL: 1.00 ± 0.00 (normalized), n = 3 (independent experiments); Control (Rap): 2.46 ± 0.23 (normalized), n = 3 (independent experiments); Control (BafA1): 2.29 ± 0.10 (normalized), n = 3 (independent experiments); $F_{(2,6)}$ = 30.13, p = 0.0007, analyzed by One-way ANOVA followed by Tukey HSD post hoc test. SCAMP5 KD (CTL): 1.00 ± 0.00 (normalized), n = 3 (independent experiments); SCAMP5 KD (Rap): 2.42 ± 0.28 (normalized), n = 3 (independent experiments); SCAMP5 KD (BafA1): 2.42 ± 0.35 (normalized), n = 3 (independent experiments); $F_{(2,6)}$ = 10.07, p = 0.0121, analyzed by One-way ANOVA followed by Tukey HSD post hoc test. Values are indicated as mean ± SEM. *p < 0.05, **p < 0.01, ***p < 0.001.

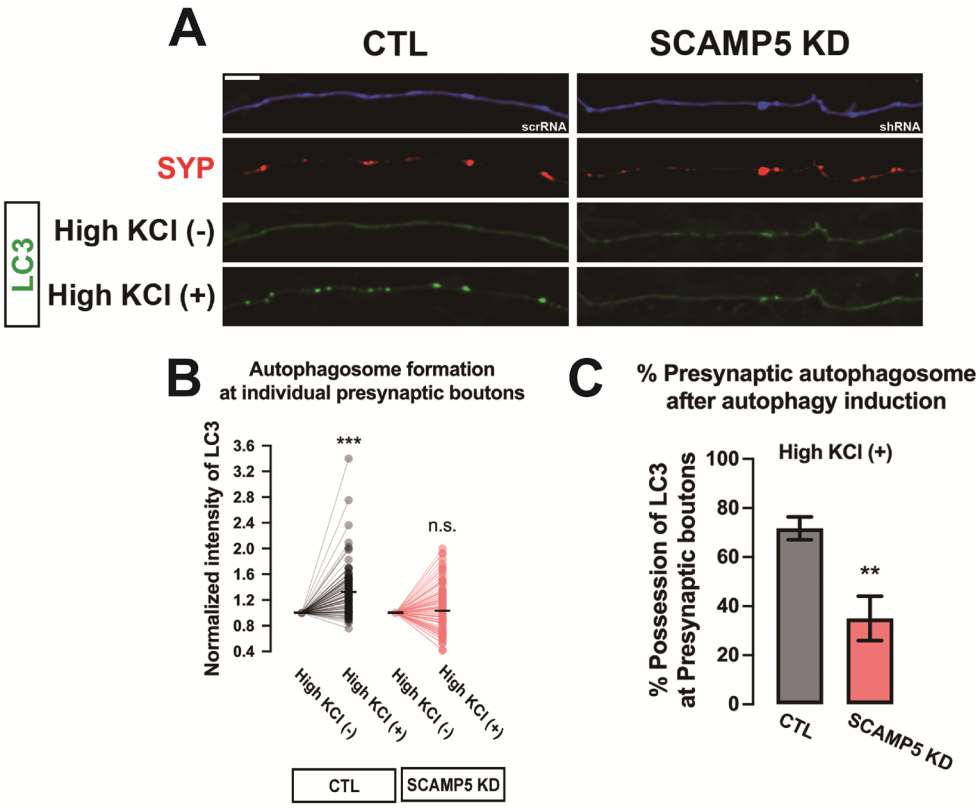

Figure 5. Downregulation of SCAMP5 leads to impaired activity-dependent autophagosome formation at presynaptic boutons

(A) Representative images of cultured rat hippocampal neurons co-transfected with mTagBFP2-scrRNA or shRNA of SCAMP5, mCherry-Synaptophysin (SYP; presynaptic bouton marker), and EGFP-LC3 (autophagosome marker) with or without treatment of high KCl for autophagy induction. Scale bar: 5 μm. (B) Quantification of the normalized relative intensity of LC3 protein expression in CTL and SCAMP5 KD neurons with or without treatment of high KCl treatment, CTL: high KCl (−): 1.000 ± 0.000 (normalized), high KCl (+): 1.326 ± 0.038, n = 104 (boutons, 6 coverslips); $p < 0.0001$, analyzed by Student's t-test, SCAMP5 KD: high KCl (−): 1.000 ± 0.000 (normalized), high KCl (+): 1.033 ± 0.037, n = 104 (boutons, 6 coverslips); p= 0.367, analyzed by Student's t-test. Values are indicated as mean ± SEM. (C) Percentage of LC3 possession at presynaptic boutons in control and SCAMP5 KD neurons with high KCl treatment, Control: 71.72 ± 4.67, n = 5 (coverslips); SCAMP5 KD: 35.00 ± 9.04, n = 5 (coverslips); p = 0.0069, analyzed by Student's t-test. Values are indicated as mean ± SEM. **$p < 0.01$, ***$p < 0.001$. CTL: control;

KD: knockdown; scrRNA: scrambled RNA; shRNA: short hairpin RNA.

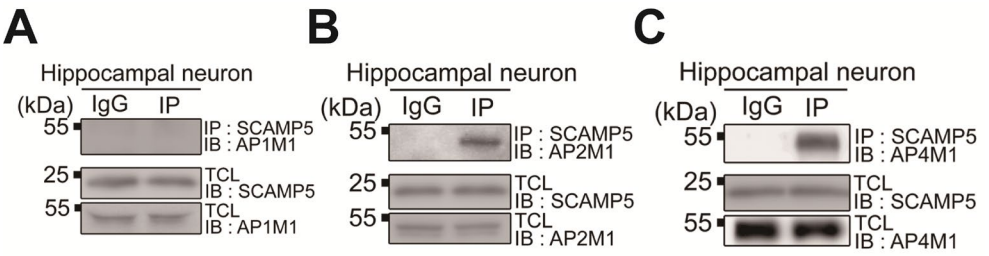

Figure 6. Identification of SCAMP5-AP4M1 interaction in the rat hippocampal neuron lysates.

(A) Rat hippocampal neuron was lysed and immunoprecipitated using anti-SCAMP5 (2nd lane) or IgG (1st lane). AP1M1 band was detected using anti-AP1M1 antibody. (B) Rat hippocampal neuron was lysed and immunoprecipitated using anti-SCAMP5 (2nd lane) or IgG (1st lane). AP2M1 band was detected using anti-AP2M1 antibody. (C) Rat hippocampal neuron was lysed and immunoprecipitated using anti-SCAMP5 (2nd lane) or IgG (1st lane). AP4M1 band was detected using anti-AP4M1 antibody. IgG: immunoglobulin; IP: immunoprecipitation.

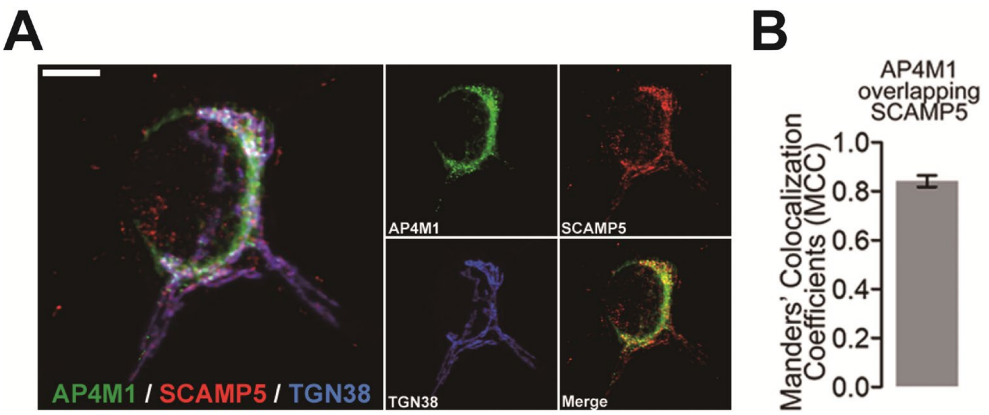

Figure 7. Identification of SCAMP5 and AP4M1 localization in the rat hippocampal neuron.

(A) Rat hippocampal neurons were subjected to immunostaining using anti-SCAMP5 antibody to detect endogenous SCAMP5. AP4M1-GFP was transfected into the rat hippocampal neuron. Scale bar: 5 μm. (B) Mander's colocalization coefficients of SCAMP5 overlapping to AP4M1, AP4M1 overlapping SCAMP5: 0.84 ± 0.05, n = 5 (coverslips). Values are indicated as mean ± SEM.

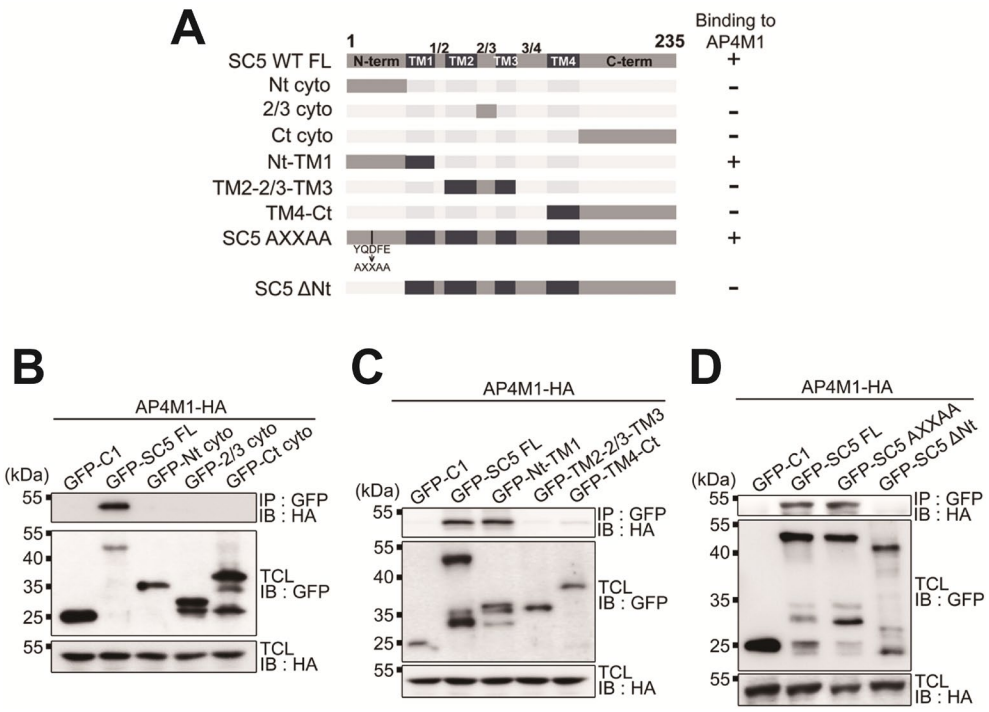

Figure 8. Identification of AP4M1-interacting domain of SCAMP5.
(A) A schematic illustration was used to depict the different domain regions of SCAMP5 employed in the experiments, with "+" or "-" markings on the right side to indicate whether a fragment or mutant of SCAMP5 was binding with AP4M1. Nt: N-terminal region; TM: transmembrane domain; 2/3: 2/3 loop domain; Ct: C-terminal region; cyto: cytoplasmic domain (B-D) AP4M1-HA and GFP-tagged various SCAMP5 fragments were expressed in HEK-293T cells, followed by cell lysis and immunoprecipitation using anti-GFP antibody, and detection of immunoprecipitated proteins with anti-HA antibody. IP: immunoprecipitation; IB: immunoblotting; TCL: total cell lysate.

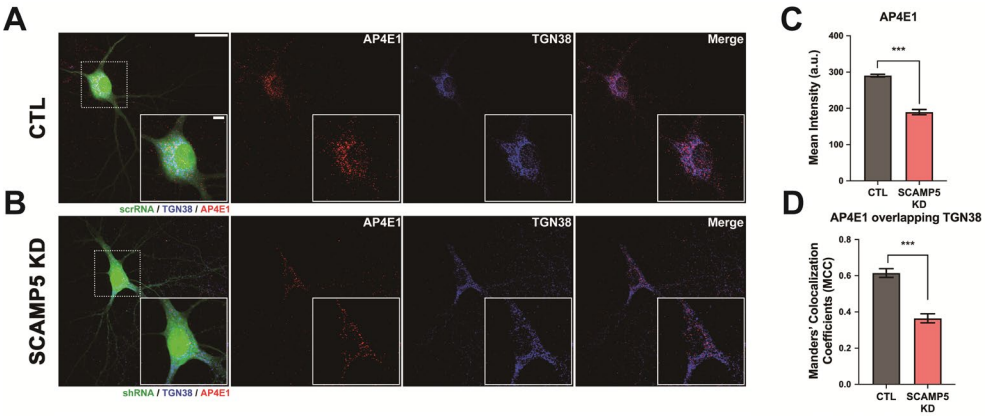

Figure 9. The absence of SCAMP5 or AP4M1 disrupts the localization of the AP4 at the trans-Golgi network.
(A-B) Representative images of cultured rat hippocampal neurons transfected with scrRNA or shRNA for SCAMP5 KD, followed by immunostaining with anti-AP4E1 and anti-TGN38 antibodies. Scale bar: 25 μm; 5 μm. (C) AP4M1 intensity acquired from CTL and SCAMP5 KD neurons, CTL: 290.10 ± 1.42, n = 7 (coverslips); SCAMP5 KD: 189.54 ± 2.72, n = 7 (coverslips); $p < 0.0001$, analyzed by Student's t-test. Values are indicated as mean ± SEM. (D) Mander's colocalization coefficients of AP4E1 overlapping to TGN38, CTL: 0.61 ± 0.01, n = 6 (coverslips); SCAMP5 KD: 0.36 ± 0.01, n = 6 (coverslips); $p < 0.0001$, analyzed by Student's t-test. Values are indicated as mean ± SEM. ***$p < 0.001$. CTL: control; KD: knockdown; scrRNA: scrambled RNA; shRNA: short hairpin RNA.

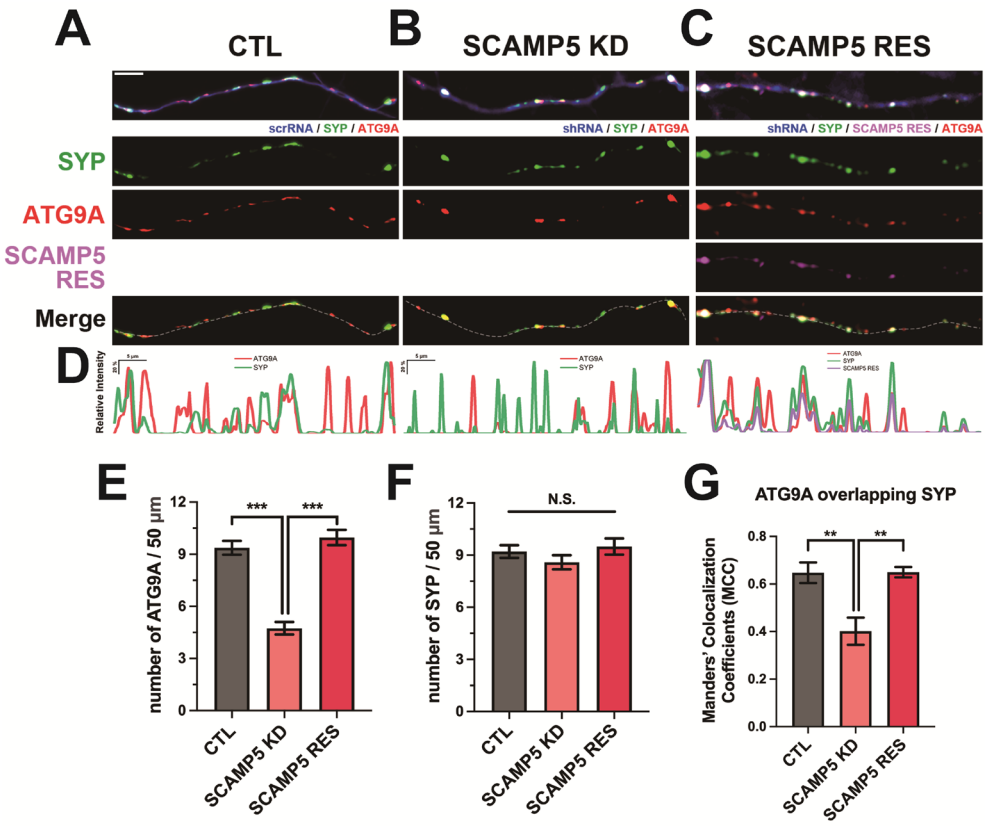

Figure 10. Axonal trafficking and presynaptic localization of overexpressed ATG9A were impaired upon knockdown of SCAMP5. (A–C) Representative images of cultured rat hippocampal neurons co-transfected with mTagBFP2-scrRNA or shRNA of SCAMP5, GFP-Synaptophysin (SYP; presynaptic bouton marker), RFP-ATG9A, and HA-shRNA-resistant form of SCAMP5. Scale bar: 5 µm. (D) Fluorescent intensity profiles of the respective protein along the axon. (E) Quantification of the number of ATG9A protein puncta along a 50 µm axon, Control: 9.37 ± 0.40, n = 38 (axons, 10 coverslips); SCAMP5 KD: 4.74 ± 0.36, n = 27 (axons, 10 coverslips); SCAMP5 RES: 9.96 ± 0.47, n = 26 (axons, 10 coverslips); $F_{(2,88)} = 45.87$, $p < 0.0001$, analyzed by One-way ANOVA followed by Tukey HSD post hoc test. Values are indicated as mean ± SEM. (F) Quantification of the number of SYP protein puncta along a 50 µm axon, Control: 9.21 ± 0.36, n = 38 (axons, 10 coverslips); SCAMP5 KD: 8.59 ± 0.40, n = 27 (axons, 10 coverslips); SCAMP5 RES: 9.50 ± 0.47, n = 26 (axons, 10 coverslips); $F_{(2,88)} = 1.1$, $p = 0.3204$, analyzed by One-way ANOVA followed by Tukey HSD post hoc test. Values are indicated as mean ± SEM. (G) Mander's colocalization coefficients of ATG9A

overlapping to SYP, CTL: 0.65 ± 0.04, n = 7 (coverslips); SCAMP5 KD: 0.40 ± 0.06, n = 7 (coverslips); SCAMP5 RES: 0.65 ± 0.02, n = 7 (coverslips); $F_{(2,28)} = 10.79$, $p = 0.0008$, analyzed by One-way ANOVA followed by Tukey HSD post hoc test. Values are indicated as mean ± SEM. $^{**}p < 0.01$, $^{***}p < 0.001$. CTL: control; KD: knockdown; scrRNA: scrambled RNA; shRNA: short hairpin RNA.

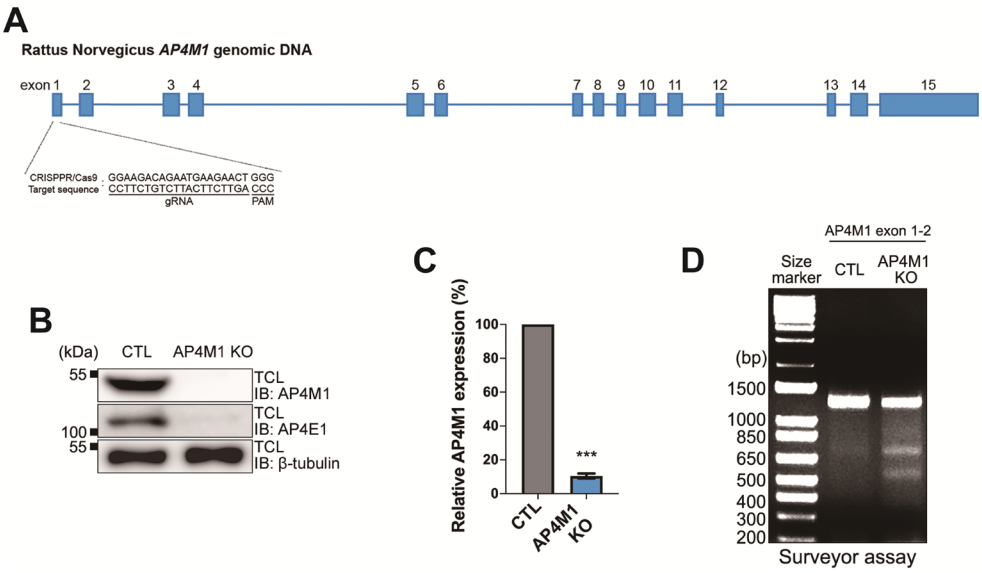

Figure 11. Validation of CRISPR/Cas9-mediated protein knockout of AP4M1

(A) A schematic illustration was utilized to illustrate the CRISPR/Cas9 targeting of the exon of rat and mouse AP4M1, and a 20-nucleotide sgRNA and PAM sequence were cloned into px458. (B) HT-22 cells were transfected with AP4M1 KO construct, and subsequently underwent cell lysis and immunoblotting with the respective antibody. (C) Normalized relative band intensity of AP4M1 protein expression, Control: 100.00 ± 0.00 (normalized), n = 3 (independent experiments); AP4M1 KO: 10.51 ± 0.87, n = 3 (independent experiments); p = 2.41E-07, analyzed by Student's t-test. Values are indicated as mean ± SEM. ***p < 0.001. (D) Validation of AP4M1 genomic DNA cleavage by CRISPR/Cas9 system by surveyor assay. KO: knockout

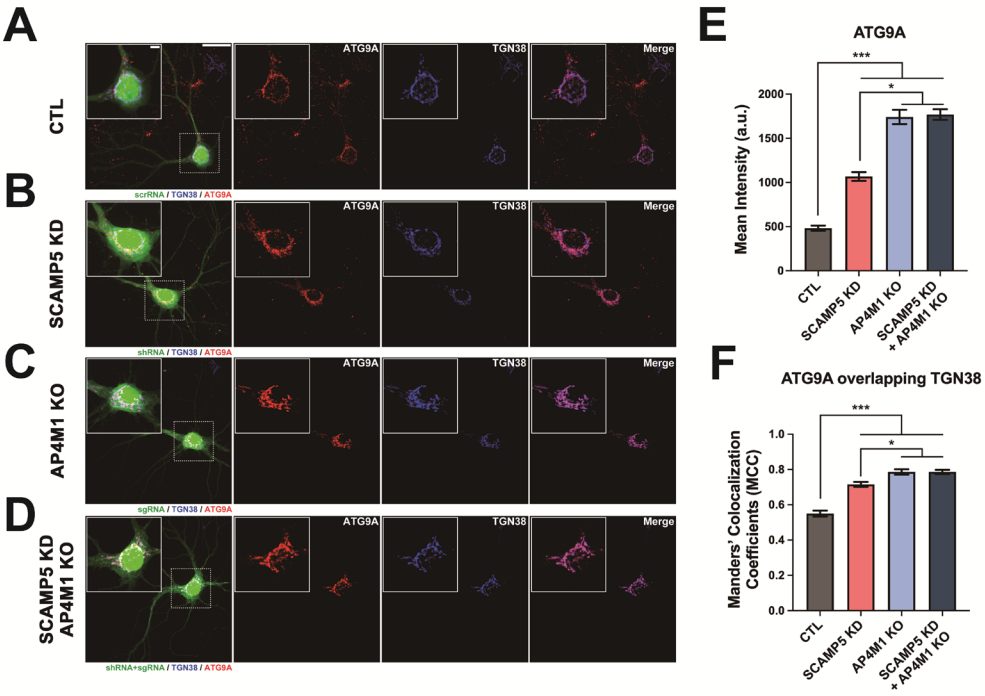

Figure 12. The accumulation of ATG9A within the TGN is observed in both SCAMP5 knockdown and AP4M1 knockout neurons.
(A–D) Representative images of cultured rat hippocampal neurons transfected with scrRNA, shRNA for SCAMP5 KD or sgRNA for AP4M1 KO, followed by immunostaining with anti–ATG9A and anti–TGN38 antibodies. Scale bar: 25 μm; 5 μm. **(E)** ATG9A intensity acquired from CTL, SCAMP5 KD, AP4M1 KO, and SCAMP5 KD + AP4M1 KO neurons, CTL: 482.00 ± 12.04, n = 6 (coverslips); SCAMP5 KD: 1067.64 ± 20.17, n = 6 (coverslips); AP4M1 KO: 1741.68 ± 33.15, n = 6 (coverslips); SCAMP5 KD + AP4M1 KO: 1769.07 ± 24.76, n = 6 (coverslips); $F_{(3,20)} = 111.3$, $p < 0.0001$, analyzed by One–way ANOVA followed by Tukey HSD post hoc test. **(F)** Mander's colocalization coefficients of ATG9A overlapping to TGN38, Control: 0.550 ± 0.007, n = 6 (coverslips); SCAMP5 KD: 0.716 ± 0.006, n = 6 (coverslips); AP4M1 KO: 0.786 ± 0.006, n = 6 (coverslips); SCAMP5 KD + AP4M1 KO: 0.786 ± 0.005, n = 6 (coverslips); $F_{(3,20)} = 58.24$, $p < 0.0001$, analyzed by One–way ANOVA followed by Tukey HSD post hoc test. Values are indicated as mean ± SEM. *p < 0.05. ***p < 0.001. CTL: control; KD: knockdown; KO: knockout; scrRNA: scrambled RNA; shRNA: short hairpin RNA; sgRNA: single guide RNA.

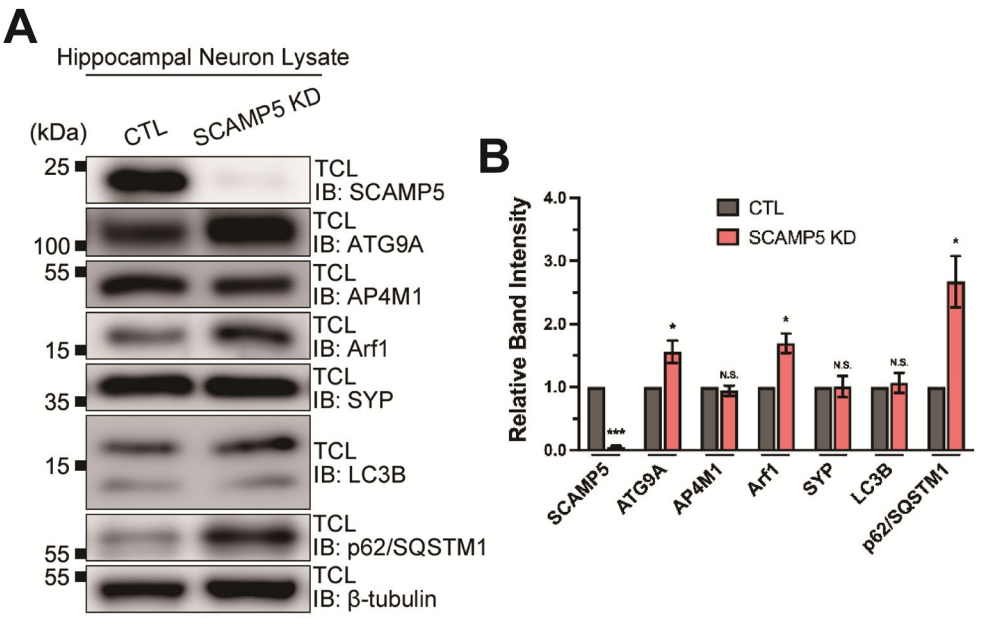

Figure 13. The level of ATG9A protein expression is slightly increased in SCAMP5 KD neurons.

(A) Cultured hippocampal neurons were subjected to treatment with AAV containing SCAMP5 scrRNA (CTL) or shRNA (SCAMP5 KD), followed by lysing the cells for immunoblotting analysis with respective antibodies. **(B)** Normalized relative band intensity of relative protein expression, SCAMP5: CTL: 1.000 ± 0.000 (normalized), n = 3 (independent experiments); SCAMP5 KD: 0.051 ± 0.020, n = 3 (independent experiments); $p < 0.0001$; ATG9A: CTL: 1.000 ± 0.000 (normalized), n = 3 (independent experiments); SCAMP5 KD: 1.560 ± 0.176, n = 3 (independent experiments); $p = 0.034$; AP4M1: CTL: 1.000 ± 0.000 (normalized), n = 3 (independent experiments); SCAMP5 KD: 0.942 ± 0.080, n = 3 (independent experiments); $p = 0.512$; Arf1: CTL: 1.000 ± 0.000 (normalized), n = 3 (independent experiments); SCAMP5 KD: 1.70 ± 0.153, n = 3 (independent experiments); $p = 0.010$; SYP: CTL: 1.000 ± 0.000 (normalized), n = 3 (independent experiments); SCAMP5 KD: 1.009 ± 0.169, n = 3 (independent experiments); $p = 0.960$; LC3B: CTL: 1.000 ± 0.000 (normalized), n = 3 (independent experiments); SCAMP5 KD: 1.068 ± 0.065, n = 3 (independent experiments); $p = 0.694$; p62/SQSTM1: CTL: 1.000 ± 0.000 (normalized), n = 3 (independent experiments); SCAMP5 KD: 2.672 ± 0.401, n = 3 (independent experiments); $p = 0.015$, analyzed by Student's t−test. Values are indicated as mean ± SEM. $*p < 0.05$, $***p < 0.001$.

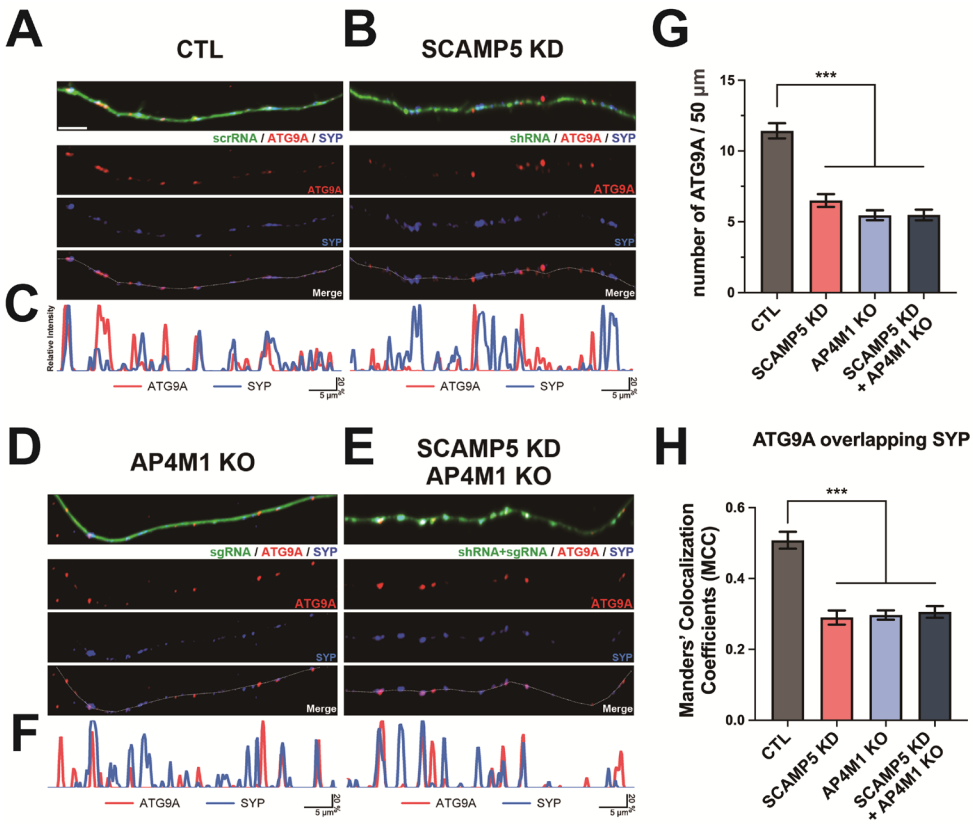

Figure 14. The accumulation of ATG9A within the TGN is observed in both SCAMP5 knockdown and AP4M1 knockout neurons.
(A, B, D, E) Representative images of cultured rat hippocampal neurons transfected mTagBFP2-scrRNA, shRNA for SCAMP5 KD or sgRNA for AP4M1 KO with mCherry-Synaptophysin (SYP; presynaptic bouton marker), followed by immunostaining with anti-ATG9A antibody. Scale bar: 5 μm. (C, F) Fluorescent intensity profiles of the respective protein along the axon. (G) Quantification of the number of ATG9A protein puncta along a 50 μm axon, CTL: 11.42 ± 0.11, n = 26 (axons, 8 coverslips); SCAMP5 KD: 7.14 ± 0.09, n = 26 (axons, 8 coverslips); AP4M1 KO: 5.46 ± 0.68, n = 26 (axons, 8 coverslips); SCAMP5 KD + AP4M1 KO: 6.14 ± 0.07, n = 27 (axons, 8 coverslips); $F_{(3,101)} = 42.91$, $p < 0.0001$, analyzed by One-way ANOVA followed by Tukey HSD post hoc test. (H) Mander's colocalization coefficients of ATG9A overlapping to SYP, Control: 0.51 ± 0.01, n = 6 (coverslips); SCAMP5 KD: 0.29 ± 0.05, n = 6 (coverslips); AP4M1 KO: 0.30 ± 0.01, n = 6 (coverslips); SCAMP5 KD + AP4M1 KO: 0.31 ± 0.04, n = 6 (coverslips); $F_{(3,20)} = 31.69$, $p < 0.0001$, analyzed by One-way ANOVA followed by Tukey HSD post hoc test. Values are indicated as mean ± SEM.

***$p<0.001$. CTL: control; KD: knockdown; KO: knockout; scrRNA: scrambled RNA; shRNA: short hairpin RNA; sgRNA: single guide RNA.

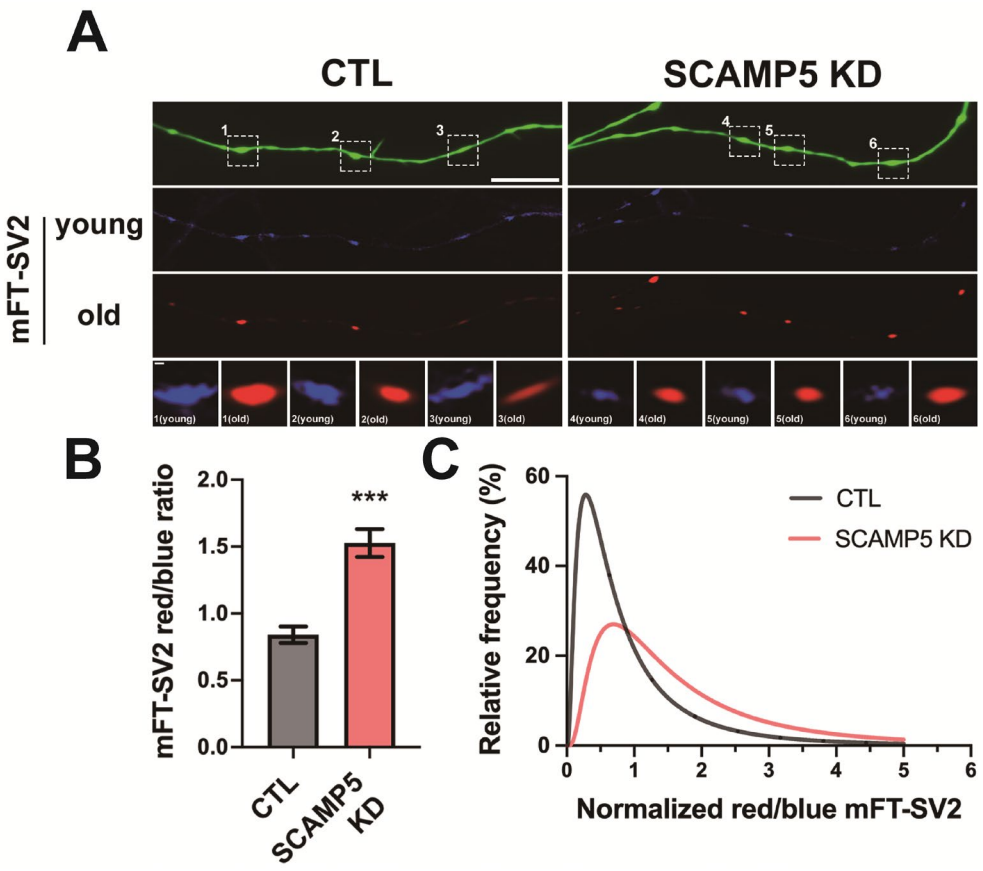

Figure 15. SCAMP5 knockdown defects in protein turnover of SV2 proteins at the presynaptic terminals.

(A) Representative images of cultured rat hippocampal neurons co-transfected with GFP-scrambled RNA or shRNA of SCAMP5, medium fluorescent timer-tagged SV2 protein (mFT-SV2). The mFT undergoes a time-dependent color change from blue to red. Scale bar: 10 μm. (B-C) Quantification of the normalized red/blue fluorescent intensities ratio, depicted in a bar graph (B), Control: 0.84 ± 0.01, n = 100 (boutons, 20 coverslips); SCAMP5 KD: 1.53 ± 0.01, n = 100 (boutons, 20 coverslips); p = 2.80E-08, analyzed by Student's t-test. Values are indicated as mean ± SEM. ***p<0.001, and as a histogram (C). CTL: control; KD: knockdown.

Discussion

In the present study, I proved that SCAMP5/AP-4/ATG9A interaction regulates the presynaptic autophagy pathway in rat hippocampal neurons. Through a series of experiments, I demonstrated that AP-4 directly binds to SCAMP5, which in turn regulates the recruitment of AP-4 into the TGN. Defects in SCAMP5 or AP-4 lead to mislocalization of the core autophagic protein ATG9A, specifically affecting its presynaptic localization and axonal trafficking, which ultimately leads to defective autophagosome formation at presynaptic boutons and impaired protein turnover of SV proteins.

SCAMP5, a membrane protein predominantly expressed in the synaptic vesicles in the brain, is considered the sole SCAMP protein involved in regulating synaptic functions, as a deficiency in SCAMP1 does not result in any synaptic function deficiencies [1, 2]. SCAMP5 plays a crucial role in SV endocytosis during high neuronal activity and is involved in the exocytic pathway in the striatum [6, 43]. SCAMP5 is also known to be a regulator of release site clearance via interaction with the AP-2 complex, highlighting the significance of SCAMP5 in the SV recycling machinery [7]. Moreover, SCAMP5 has been shown to play in regulating quantal size in glutamatergic neurons by mediating NHE6 axonal trafficking and presynaptic localization at rest and LTP state, suggesting its importance in regulating synaptic transmission [8, 44]. I showed that SCAMP5 also plays a crucial role in regulating presynaptic autophagy by controlling axonal trafficking and presynaptic localization of ATG9A, a key protein involved in autophagy. These findings underscore the multifaceted role of SCAMP5 in regulating synaptic function and protein dynamics at the presynaptic level.

Previous studies have demonstrated that all five AP complexes(AP-1~5) are primarily localized to the TGN and play a crucial role in the export and trafficking of transmembrane proteins to various destinations, including the clathrin-coated vesicles, endosome, and lysosome [11, 13, 45]. The recruitment of AP complexes to the TGN is important for proper cargo trafficking and synaptic functions. For instance, in yeast, the recruitment of AP-1 to the TGN is facilitated by HEAT repeat-containing 5 (HEATR5) proteins [46]. Similarly, in mammalian cells, ADP-Ribosylation Factor 1 (ARF1) is involved in regulating the recruitment of AP-3

to the TGN membrane [47]. AP-4 is known to be associated with the TGN through direct interaction with ARF1, and this association is facilitated by interaction between ARF1 in its GTP-bound state and two subunits of AP-4(AP4E1 and AP4M1)[48]. However, the detailed mechanism of AP-4 recruitment to the TGN in neuronal cells has not been fully elucidated. This study provides evidence that the interaction between the N-terminal region of SCAMP5 and AP4M1 is crucial for the recruitment of AP-4 to the TGN in neuronal cells. ARF1 is the only protein to be responsible for the recruitment of the AP-4 to the TGN, but the relationship between ARF1 and SCAMP5 in the recruitment of AP-4 to the TGN remains unclear. Further studies are needed to determine whether ARF1 is involved in SCAMP5-mediated recruitment of AP-4.

ATG9A is the only transmembrane protein of the core autophagic machinery that plays an essential role in the initiation of phagophore expansion, which is the initial step in the formation of autophagosomes. ATG9A is mainly localized in axon terminals and is present in synaptic vesicles, where it plays important role in synapse development and synaptic autophagy[39, 49, 50]. For axonal trafficking of ATG9A, AP-4 plays a pivotal role in regulating presynaptic autophagy by facilitating the delivery of ATG9A vesicles to the synapse, and its deficiency leads to the depletion of axonal ATG9A [25, 38, 51]. Presynaptic autophagy is a crucial process for maintaining protein homeostasis and functional integrity of synaptic terminals [40, 52] and this process is important for the selective removal of damaged organelles and toxic proteins, preventing their accumulation and potential toxicity [20, 53]. My data shows that SCAMP5 and AP-4 complex is essential for the proper localization of ATG9A at presynaptic terminals, which is crucial for presynaptic autophagy.

There is a well-established correlation between presynaptic activity and synaptic vesicle protein turnover [54], and defects in synaptic autophagy can lead to abnormal synaptic activity, as autophagy is closely associated with synapses and synaptic dysfunction in diseases such as Parkinson's disease and epilepsy [55-58]. SCAMP5 is also a candidate gene of Parkinson's disease and epilepsy, as two specific mutations, R91W and G180W, in SCAMP5 have been identified in individuals with neurodevelopmental disorders characterized by autistic features and seizures, and deficiency of SCAMP5 has been linked to pediatric epilepsy and juvenile Parkinson's disease [3-5]. While

the precise mechanisms by which these mutations lead to disease are not yet fully understood, all of these diseases are associated with autophagy deficiency [56, 59, 60]. Given the critical role of SCAMP5 in regulating presynaptic autophagy, R91W and G180W mutations may indirectly affect synaptic autophagy and contribute to the pathogenesis of these diseases. Further research targeting the mutation models of SCAMP5 could potentially lead to the development of therapeutic strategies aimed at treating neurodevelopmental disorders associated with SCAMP5 mutations and autophagy dysfunction.

References

1. Fernández-Chacón, R. and T.C. Südhof, *Novel SCAMPs lacking NPF repeats: ubiquitous and synaptic vesicle-specific forms implicate SCAMPs in multiple membrane-trafficking functions.* Journal of Neuroscience, 2000. **20**(21): p. 7941-7950.
2. Ferna´ndez-Chaco´n, R., et al., *Analysis of SCAMP1 function in secretory vesicle exocytosis by means of gene targeting in mice.* Journal of Biological Chemistry, 1999. **274**(46): p. 32551-32554.
3. Hubert, L., et al., *De novo SCAMP5 mutation causes a neurodevelopmental disorder with autistic features and seizures.* Journal of medical genetics, 2020. **57**(2): p. 138-144.
4. Zhang, D., et al., *Deficiency of SCAMP5 leads to pediatric epilepsy and dysregulation of neurotransmitter release in the brain.* Human Genetics, 2020. **139**: p. 545-555.
5. Jiao, X., et al., *Identification of an identical de Novo SCAMP5 missense variant in four unrelated patients with seizures and severe neurodevelopmental delay.* Frontiers in Pharmacology, 2020. **11**: p. 599191.
6. Zhao, H., et al., *SCAMP5 plays a critical role in synaptic vesicle endocytosis during high neuronal activity.* Journal of Neuroscience, 2014. **34**(30): p. 10085-10095.
7. Park, D., et al., *Impairment of release site clearance within the active zone by reduced SCAMP5 expression causes short-term depression of synaptic release.* Cell reports, 2018. **22**(12): p. 3339-3350.
8. Lee, U., et al., *SCAMP5 plays a critical role in axonal trafficking and synaptic localization of NHE6 to adjust quantal size at glutamatergic synapses.* Proceedings of the National Academy of Sciences, 2021. **118**(2): p. e2011371118.
9. Pearse, B.M.F. and M.S. Bretscher, *Membrane recycling by coated vesicles.* Annual review of biochemistry, 1981. **50**(1): p. 85-101.
10. Hirst, J., C. Irving, and G.H. Borner, *Adaptor protein complexes AP-4 and AP-5: new players in endosomal trafficking and progressive spastic paraplegia.* Traffic, 2013. **14**(2): p. 153-164.
11. Majumder, P., et al., *AP-4 regulates neuronal lysosome composition, function, and transport via regulating export of critical lysosome receptor proteins at the trans-Golgi network.* Molecular Biology of the Cell, 2022. **33**(12): p. ar102.
12. Fuji, K., et al., *The adaptor complex AP-4 regulates vacuolar protein sorting at the trans-Golgi network by interacting with VACUOLAR SORTING RECEPTOR1.* Plant Physiology, 2016. **170**(1): p. 211-219.
13. Hirst, J., et al., *Role of the AP-5 adaptor protein complex in late endosome-to-Golgi retrieval.* PLoS biology, 2018. **16**(1): p. e2004411.

14. Abou Jamra, R., et al., *Adaptor protein complex 4 deficiency causes severe autosomal-recessive intellectual disability, progressive spastic paraplegia, shy character, and short stature.* The American Journal of Human Genetics, 2011. **88**(6): p. 788-795.
15. Moreno-De-Luca, A., et al., *Adaptor protein complex-4 (AP-4) deficiency causes a novel autosomal recessive cerebral palsy syndrome with microcephaly and intellectual disability.* Journal of medical genetics, 2011. **48**(2): p. 141-144.
16. Ebrahimi-Fakhari, D., et al., *Clinical and genetic characterization of AP4B1-associated SPG47.* American Journal of Medical Genetics Part A, 2018. **176**(2): p. 311-318.
17. Martinez-Vicente, M. and A.M. Cuervo, *Autophagy and neurodegeneration: when the cleaning crew goes on strike.* The Lancet Neurology, 2007. **6**(4): p. 352-361.
18. Mizushima, N., et al., *Autophagy fights disease through cellular self-digestion.* nature, 2008. **451**(7182): p. 1069-1075.
19. Korolchuk, V.I. and D.C. Rubinsztein, *Regulation of autophagy by lysosomal positioning.* Autophagy, 2011. **7**(8): p. 927-928.
20. Sumitomo, A. and T. Tomoda, *Autophagy in neuronal physiology and disease.* Current Opinion in Pharmacology, 2021. **60**: p. 133-140.
21. Nakatogawa, H., *Mechanisms governing autophagosome biogenesis.* Nature reviews Molecular cell biology, 2020. **21**(8): p. 439-458.
22. Imai, K., et al., *Atg9A trafficking through the recycling endosomes is required for autophagosome formation.* Journal of cell science, 2016. **129**(20): p. 3781-3791.
23. Guardia, C.M., et al., *Structure of human ATG9A, the only transmembrane protein of the core autophagy machinery.* Cell reports, 2020. **31**(13): p. 107837.
24. Mattera, R., et al., *AP-4 mediates export of ATG9A from the trans-Golgi network to promote autophagosome formation.* Proceedings of the National Academy of Sciences, 2017. **114**(50): p. E10697-E10706.
25. Ivankovic, D., et al., *Axonal autophagosome maturation defect through failure of ATG9A sorting underpins pathology in AP-4 deficiency syndrome.* Autophagy, 2020. **16**(3): p. 391-407.
26. Dobson, L., I. Reményi, and G.E. Tusnády, *CCTOP: a Consensus Constrained TOPology prediction web server.* Nucleic acids research, 2015. **43**(W1): p. W408-W412.
27. Ran, F.A., et al., *Genome engineering using the CRISPR-Cas9 system.* Nature protocols, 2013. **8**(11): p. 2281-2308.
28. Liu, L., et al., *Role of secretory carrier membrane protein SCAMP2 in granule exocytosis.* Molecular biology of the cell, 2002. **13**(12): p. 4266-4278.
29. Ferna´ndez-Chaco´n, R., et al., *SCAMP1 function in endocytosis.* Journal of Biological Chemistry, 2000. **275**(17): p. 12752-12756.
30. Thomas, P., D. Wohlford, and Q.L. Aoh, *SCAMP 3 is a novel regulator of endosomal morphology and composition.* Biochemical

and biophysical research communications, 2016. **478**(3): p. 1028-1034.
31. Singleton, D., T. Wu, and J. Castle, *Three mammalian SCAMPs (secretory carrier membrane proteins) are highly related products of distinct genes having similar subcellular distributions.* Journal of cell science, 1997. **110**(17): p. 2099-2107.
32. Hoffmann, S., et al., *Light-Activated ROS Production Induces Synaptic Autophagy.* J Neurosci, 2019. **39**(12): p. 2163-2183.
33. Hurley, J.H. and L.N. Young, *Mechanisms of autophagy initiation.* Annual review of biochemistry, 2017. **86**: p. 225-244.
34. De Tito, S., et al., *The Golgi as an assembly line to the autophagosome.* Trends in biochemical sciences, 2020. **45**(6): p. 484-496.
35. Pavel, M. and D.C. Rubinsztein, *Mammalian autophagy and the plasma membrane.* The FEBS journal, 2017. **284**(5): p. 672-679.
36. Yang, S., et al., *Presynaptic autophagy is coupled to the synaptic vesicle cycle via ATG-9.* Neuron, 2022. **110**(5): p. 824-840. e10.
37. Tsuji, T. and Y. Niida, *Development of a simple and highly sensitive mutation screening system by enzyme mismatch cleavage with optimized conditions for standard laboratories.* Electrophoresis, 2008. **29**(7): p. 1473-1483.
38. De Pace, R., et al., *Altered distribution of ATG9A and accumulation of axonal aggregates in neurons from a mouse model of AP-4 deficiency syndrome.* PLoS genetics, 2018. **14**(4): p. e1007363.
39. Park, D., et al., *Synaptic vesicle proteins and ATG9A self-organize in distinct vesicle phases within synapsin condensates.* Nature Communications, 2023. **14**(1).
40. Ivanova, D. and M.A. Cousin, *Synaptic vesicle recycling and the endolysosomal system: a reappraisal of form and function.* Frontiers in synaptic neuroscience, 2022. **14**.
41. Hoffmann-Conaway, S., et al., *Parkin contributes to synaptic vesicle autophagy in Bassoon-deficient mice.* Elife, 2020. **9**: p. e56590.
42. Subach, F.V., et al., *Monomeric fluorescent timers that change color from blue to red report on cellular trafficking.* Nature chemical biology, 2009. **5**(2): p. 118-126.
43. Noh, J.Y., et al., *SCAMP5 links endoplasmic reticulum stress to the accumulation of expanded polyglutamine protein aggregates via endocytosis inhibition.* J Biol Chem, 2009. **284**(17): p. 11318-25.
44. Lee, U., S.H. Ryu, and S. Chang, *SCAMP5 mediates activity-dependent enhancement of NHE6 recruitment to synaptic vesicles during synaptic plasticity.* Mol Brain, 2021. **14**(1): p. 47.
45. Popova, N., I. Deyev, and A. Petrenko, *Clathrin-mediated endocytosis and adaptor proteins.* Acta Naturae (англоязычная версия), 2013. **5**(3 (18)): p. 62-73.
46. Zysnarski, C.J., et al., *Adaptor protein complex-1 (AP-1) is recruited by the HEATR5 protein Laa1 and its co-factor Laa2 in yeast.* Journal of Biological Chemistry, 2019. **294**(4): p. 1410-

1419.
47. Ooi, C.E., E.C. Dell'Angelica, and J.S. Bonifacino, *ADP-Ribosylation factor 1 (ARF1) regulates recruitment of the AP-3 adaptor complex to membranes.* The Journal of cell biology, 1998. **142**(2): p. 391-402.
48. Boehm, M., R.C. Aguilar, and J.S. Bonifacino, *Functional and physical interactions of the adaptor protein complex AP-4 with ADP-ribosylation factors (ARFs).* EMBO J, 2001. **20**(22): p. 6265-76.
49. Limanaqi, F., et al., *Interdependency Between Autophagy and Synaptic Vesicle Trafficking: Implications for Dopamine Release.* Frontiers in Molecular Neuroscience, 2018. **11**.
50. Xuan, Z., et al., *The active zone protein Clarinet regulates synaptic sorting of ATG-9 and presynaptic autophagy.* PLoS Biol, 2023. **21**(4): p. e3002030.
51. Scarrott, J.M., et al., *Ap4b1-knockout mouse model of hereditary spastic paraplegia type 47 displays motor dysfunction, aberrant brain morphology and ATG9A mislocalization.* Brain Commun, 2023. **5**(1): p. fcac335.
52. Lieberman, O.J. and D. Sulzer, *The synaptic autophagy cycle.* Journal of molecular biology, 2020. **432**(8): p. 2589-2604.
53. Vijayan, V. and P. Verstreken, *Autophagy in the presynaptic compartment in health and disease.* Journal of Cell Biology, 2017. **216**(7): p. 1895-1906.
54. Jahne, S., et al., *Presynaptic activity and protein turnover are correlated at the single-synapse level.* Cell Reports, 2021. **34**(11).
55. Lee, W. and S.H. Kim, *Autophagy at synapses in neurodegenerative diseases.* Archives of pharmacal research, 2019. **42**: p. 407-415.
56. Prieto, G.A. and C.W. Cotman, *Early bioenergetic and autophagy impairments at the Parkinson' s disease synapse.* Brain, 2022. **145**(6): p. 1877-1879.
57. Vijayan, V. and P. Verstreken, *Autophagy in the presynaptic compartment in health and disease.* J Cell Biol, 2017. **216**(7): p. 1895-1906.
58. Zhu, H., W. Wang, and Y. Li, *Molecular Mechanism and Regulation of Autophagy and Its Potential Role in Epilepsy.* Cells, 2022. **11**(17).
59. Deng, Z., et al., *Autophagy deficiency in neurodevelopmental disorders.* Cell & Bioscience, 2021. **11**(1): p. 214.
60. Zhu, Y., et al., *Autophagy in childhood neurological disorders.* Developmental Medicine & Child Neurology, 2019. **61**(6): p. 639-645.

요약 (국문초록)

Secretory carrier membrane protein 5 (SCAMP5)는 뇌와 시냅스 소낭에 주로 존재하는 막단백질로 뉴런의 시냅스 기능 조절에 핵심적인 역할을 담당한다. 최근 연구에 따르면 SCAMP5는 시냅스 소낭의 endo/exocytosis와 신경 축삭으로의 단백질 수송 및 시냅스전세포 단백질 위치화에 관여한다고 알려졌다. 하지만 SCAMP5는 시냅스 소낭 외, 골지망 (Golgi network)에도 많이 존재하는데 시냅스 기능을 조절하는 SCAMP5가 왜 골지망에 분포돼있는지 알려진 바가 부족하다.

본 연구는 SCAMP5 결핍 뉴런의 시냅스전세포에서 자가포식소체 형성에 문제가 생기는 현상 발견으로부터 시작됐다. 공동면역침강법과 단백질-단백질 결합 검출 결과, SCAMP5는 Adapter protein 4 (AP-4)의 μ4 아단위 (AP4M1)와 직접 연결돼 있으며 해당 결합은 SCAMP5의 N-terminal 영역과 직접적 연관이 있음을 발견했다. 또한 면역염색 기법과 형광 이미징을 통해 SCAMP5와 AP4M1의 상호작용이 AP-4가 후기골지망 (trans-Golgi network; TGN)으로 위치하는 현상에 중요한 역할을 한다는 것을 밝혔다. AP-4는 TGN에서 단백질 분류 및 패킹을 담당하며 이는 단백질 소낭을 통한 단백질 운송에 중요한 역할을 한다. 그 중 자가포식에 중요한 단백질 중 하나인 ATG9A도 AP-4를 통해 TGN에서 빠져나가 필요한 위치로 수송된다. 백서해마세포에 shRNA와 CRISPR/Cas9 시스템을 통한 SCAMP5 발현 저하 유도 혹은 SCAMP5/AP4M1의 결합을 저해하게 될 경우 신경 축삭으로 수송되는 ATG9A 포함 소낭이 유의미하게 줄어들며 시냅스전세포로 위치화 되는 정도도 감소한다. 이는 시냅스 전 말단에서 유발되는 자가포식 현상 결핍과 시냅스 소낭 관련 단백질 대사회전의 감소로 이어진다.

해당 결과들은 SCAMP5와 AP-4의 직접적 상호 작용이 AP-4가 TGN으로 위치되는 것에 중요한 역할을 하며, 이는 ATG9A의 신경 축삭으로의 수송과 시냅스 위치화에 영향을 주는 것을 나타낸다. SCAMP5와 자가포식 결핍 현상 모두 신경 발달장애와 깊은 연관이 있는 것을 고려할 때, 추후 연구에서는 해당 단백질 복합체가 병리 발생의 분자적 메커니즘에 어떤 연관이 있는지 밝혀낼 것을 기대한다.

주요어: SCAMP5, AP-4, ATG9A, axonal trafficking, 시냅스전뉴런, 자가포식작용

학번: 2021-22014
